Autoionizing states in the photoionization of the $3s^2 3p^4\ ^3P^e$ ground state of sulfur

S. S. Tayal
Department of Physics and Astronomy, Louisiana State University, Baton Rouge, Louisiana 70803-4001
(Received 13 April 1987; revised manuscript received 14 March 1988)

The partial and total photoionization cross sections for the S($3s^2 3p^4\ ^3P^e$) ground state, leaving the residual S^+ ions in the lowest three $3s^2 3p^3\ ^4S^o, ^2D^o, ^2P^o$ LS states, are calculated in both the dipole length and velocity forms. Extensive configuration-interaction wave functions are used to describe both the initial bound S state and the final continuum S^+ states. The prominent features in the cross sections are the autoionization Rydberg series converging to $S^+(3s^2 3p^3\ ^2D^o, ^2P^o)$ excited-state thresholds. The parameters of these autoionizing levels are presented. The present results are compared with the available experimental measurements and other calculations.

I. INTRODUCTION

The photoionization spectrum of sulfur has been studied in the past by both theoretical and experimental groups. The sulfur absorption spectrum was reported by Tondello[1] for the energy regions below and above the ionization threshold. He measured the absolute value of the cross section for the photoionization of the ground state of sulfur for photon energies from the threshold at 1196.7 Å($\simeq 0.7614$ Ry) to 900 Å ($\simeq 1.0124$ Ry) using the flash-pyrolysis method. Sarma and Joshi[2] studied the photoionization spectrum of sulfur using a method similar to Tondello's.[1] They modified and extended Tondello's spectrum, particularly in the region between 1090 and 1000 Å. Gibson *et al.*[3] observed the photoionization spectrum of sulfur in the region between the first ionization threshold and 950 Å. They found that the autoionization features of the $3p^3(^2D^o)nd\ ^3D^o$ levels are broad while that of the $3p^3(^2D^o)nd\ ^3S^o, ^3P^o$ levels are narrow. Their results are in good agreement with the measurements of Tondello.[1] However, they have reversed the designation given by Tondello to the $3p^3(^2D^o)nd\ ^3S^o$ and $3p^3(^2D^o)ns\ ^3D^o$ levels. They supported their new assignment of the levels mainly on the basis of the quantum defects of the two series. More recently, Joshi *et al.*[4] obtained the photoabsorption spectrum of sulfur in the 1220–840-Å range. They gave a detailed comparison of the line list obtained in their measurement with that of Tondello,[1] Sarma and Joshi,[2] and Gibson *et al.*[3] The emission spectrum of sulfur has been studied by a number of experimental groups[5–7] in the energy regions below and above the first ionization limit. Kaufman[7] measured 114 lines of atomic sulfur between 1157 and 2169 Å involving transitions to the levels of the ground configuration. On the theoretical side, the photoionization cross section of sulfur has been calculated by Conneely *et al.*[8] using the close-coupling approximation. They have reported the parameters of the resonance series in the photoionization of sulfur from the ground state. Mendoza calculated some preliminary results, as quoted by Berrington and Taylor,[9] using the linear-algebraic and R-matrix methods. Mendoza and Zeippen[10] have very recently published the photoionization cross sections of the ground states of Si, P, and S.

The study of the photoionization of sulfur is of considerable interest because of its applications in astrophysics. Sulfur has recently been discovered in the plasma of the Jupiter satellite Io.[11,12] Spectroscopic measurements indicate that sulfur and oxygen dominate the torus plasma of the Jupiter satellite Io. Furthermore, the study of the photoabsorption spectrum of sulfur can be interesting due to the open-shell features of the sulfur atom and the correlation effects can be quite important. Recently, Tayal *et al.*[13] considered the electron-impact excitation of singly ionized sulfur using the R-matrix method.[14] In this paper the total and partial cross sections for the photoionization of the $3s^2 3p^4\ ^3P^e$ ground state of sulfur atom are presented for photon energies from the first $S^+(3s^2 3p^3\ ^4S^o)$ ionization threshold to 1.8 Ry. Results have been calculated in both dipole length and dipole velocity approximations using the R-matrix method of photoionization.[15] In this method the correlation effects in the final continuum states and in the initial bound state are included in a consistent manner by using similar R-matrix expansions for both states. The LS coupling scheme is used in the present work. The $3s^2 3p^4$ ground configuration of sulfur gives rise to the $^3P^e$, $^1D^e$, and $^1S^e$ terms and the excitation of $3p$ electrons into Rydberg orbitals produces $3s^2 3p^3 nl$ Rydberg series with $S^+(3s^2 3p^3\ ^4S^o, ^2D^o, ^2P^o)$ core. The $^3S^o$, $^3P^o$, and $^3D^o$ final states are allowed by dipole selection rules for the photoionization of sulfur from the $3s^2 3p^4\ ^3P^e$ ground state. The total photoionization cross section is obtained by adding the contributions of the final states. The cross sections are dominated by the $3p^3(^2D^o)nd\ ^3S^o, ^3D^o$ and $3p^3(^2D^o)ns\ ^3D^o$ Rydberg series of resonances occurring below the $^2D^o$ ionization threshold and the $3p^3(^2P^o)ns\ ^3P^o$ and $3p^3(^2P^o)nd\ ^3P^o, ^3D^o$ Rydberg series of resonances which occur below the $^2P^o$ threshold. The $^3P^o$ series converging to the $^2D^o$ threshold cannot autoionize into the continuum associated with the $^4S^o$ limit. The $3p^3(^2D^o)ng\ ^3D^o$ series of resonances converging to $^2D^o$ threshold is very weakly coupled to the initial state to give rise to any observable effects.

In Sec. II the initial- and final-state wave functions are described; the details of R-matrix calculations are presented in Sec. III. The results of the partial and total photoionization cross sections and the autoionized levels are presented in Sec. IV, where they are discussed and compared with the experimental measurements and other theoretical calculations.

II. THE INITIAL- AND FINAL-STATE WAVE FUNCTIONS

In the R-matrix formulation of atomic photoionization, the initial bound state and the final continuum states are represented consistently by R-matrix expansions in terms of ionic states. The three lowest $S^+(3s^23p^3\ {}^4S^o, {}^2D^o, {}^2P^o)$ states are included in the present calculation. These ionic states are described by configuration-interaction (CI) wave functions constructed from nine orthogonal one-electron orbitals $(1s, 2s, 2p, 3s, 3p, 3d, 4s, 4p, 4f)$. The $1s$, $2s$, $2p$, $3s$, and $3p$ radial functions are those of the $3s^23p^3\ {}^4S^o$ ground state of S^+ ion given by Clementi and Roetti.[16] The $3d$, $4s$, $4p$, and $4f$ correlation functions are obtained using the CIV3 program of Hibbert.[17] In order to improve the energies of the ionic states, a number of test calculations were performed to obtain $3d$, $4s$, $4p$, and $4f$ radial orbitals using the different criteria of optimization and number of basis functions. In our final calculation the $3d$ and $4s$ orbitals are optimized on the $3s^23p^3\ {}^4S^o$ state while $4p$ and $4f$ orbitals are chosen to improve the excited-state thresholds $^2P^o$ and $^2D^o$, respectively. The parameters of the non-Hartree-Fock radial functions are given in Table I. In order to account for the important correlation effects in the ionic wave functions, up to three-electron excitations are considered. The three-electron excitations giving rise to the configurations $3s3p3d^3$ which correspond to the "internal correlations" are found to be important. However, in the final calculation all the configurations with smaller coefficients (<0.007) are dropped and a total of 40 configurations are used for the description of three ionic states. In Table II a list of configurations used for each state is given. The coefficient of each configuration in the CI expansions is given below the configuration. It is easily seen from this table that the CI effects are very important. All these configurations contain a common $1s^22s^22p^6$ core. The calculated ionic energies (in a.u.) relative to the ground state are presented in Table III where they are compared with experiment.[18] The calculated excited-state thresholds for S^+ $3s^23p^3\ {}^2D^0$ and $^2P^o$ states differ from the measured thresholds by about 12%.

The initials $S(^3P^e)$ state is represented as a bound state of the electron plus S^+ ion system. The total wave function for the $N+1$ electrons of the system is expanded in an internal region surrounding the atom in terms of R-matrix basis functions defined by

$$\Psi_k(X_1,\ldots,X_{N+1})=A\sum_{i,j}c_{ijk}\Phi_i(X_1,\ldots,X_N\hat{r}_{N+1},\sigma_{N+1})u_{ij}(r_{N+1})+\sum_j d_{jk}\phi_j(X_1,\ldots,X_{N+1})\ . \tag{1}$$

where A is the antisymmetrization operator, Φ_i are channel functions consisting of the wave function for the residual ion coupled with the spin-angle function of the $(N+1)$th electron to give an eigenstate of L, S, and π. The ϕ_j are $(N+1)$-electron bound configurations with the same L, S, and π. The u_{ij} are the continuum orbitals obtained by solving the zero-order radial differential equation

$$\left[\frac{d2}{dr^2}-\frac{l_i(l_i+1)}{r^2}+V(r)+k_j^2\right]u_{ij}=\sum_k\lambda_{ijk}P_k(r)\ . \tag{2}$$

Satisfying the boundary condition at $r=0$

$$u_{ij}(0)=0 \tag{3}$$

and at the R-matrix boundary radius $r=a$

$$\frac{a}{u_{ij}}\frac{du_{ij}}{dr}=b\ . \tag{4}$$

$V(r)$ is a zero-order potential which is chosen to be the ground-state static potential and the constant b is chosen to be zero. Lagrange undetermined multipliers λ_{ijk} ensure that the continuum orbitals are orthogonal to bound orbitals $P_k(r)$ with the same angular symmetry.

TABLE I. Parameters for the bound orbitals used in the calculation. Each orbital is a sum of Slater-type orbitals.

Orbital	Coefficient	Power of r	Exponent
$3d$	3.711 97	3	1.861 68
$4s$	1.929 42	1	10.650 33
	−10.428 66	2	2.099 29
	43.669 92	3	1.855 58
	−63.097 14	4	2.413 85
$4p$	4.167 04	2	0.783 18
	−10.814 71	3	1.072 91
	5.762 31	4	1.330 72
$4f$	2.522 18	4	1.995 16

III. CALCULATIONS

In the present work all the continuum channels associated with the three lowest states of the S^+ residual ion are included. Thus the number of channels for $^3S^o$, $^3P^o$, and $^3D^o$ continuum states are 2, 3, and 5, respectively. The calculations are carried out using the R-matrix program of Berrington *et al.*[19] The strong CI effects in the initial- and final-state wave functions are allowed by a superposition of $(N+1)$-electron configurations which are constructed from the bound orbitals given in Table I. A boundary radius $r=13.8$ a.u. for the internal spherical region is chosen which is large enough to contain these configurations. Fifteen continuum orbitals for each an-

TABLE II. Configurations used for each state in the present calculation. The numbers below the configurations give their weights.

State	Configuration, weight				
$3p^3\,^4S^o$	$3s^23p^3$	$3s3p^3(^2D^o)3d$	$3s3p^3(^4S^o)^3S^o4s$	$3s^23p3d^2(^3P)$	$3s3p3d^3(^2P)$
	−0.972 40	0.204 25	−0.014 74	0.091 04	−0.018 48
	$3s3p3d^3(^4P)$	$3s^23p^2(^3P)4p$	$3p^3(^4S^o)3d^2(^1S)$	$3s3p^3(^4S^o)^5S^o4s$	
	−0.012 25	0.012 94	0.058 61	0.011 06	
$3p^3\,^2D^o$	$3s^23p^3$	$3s3p^3(^2D^o)^1D^o3d$	$3s3p^3(^4S^o)3d$	$3s3p^3(^2D^o)^3D^o3d$	$3s^23p3d^2(^1D)$
	0.969 41	0.136 49	−0.116 91	−0.085 28	−0.083 22
	$3s^23p3d^2(^3P)$	$3s^23p^2(^3P)4p$	$3s^23p^2(^3P)4f$	$3s^23p^2(^1D)4f$	$3p^3(^2D^0)3d^2(^1S)$
	0.063 79	0.019 22	0.059 37	0.044 90	−0.058 44
	$3s3p^3(^2P^o)^3P^o3d$	$3s^23p3d^2(^3F)$	$3s3p^3(^2D^o)^1D^o4s$		
	0.014 31	0.009 56	0.008 06		
$3p^3\,^2P^o$	$3s^23p^3$	$3p^5$	$3s^23p3d^2(^3P)$	$3s^23p3d^2(^1S)$	$3s^23p3d^2(^1D)$
	0.960 15	−0.165 28	0.066 44	−0.119 52	0.075 66
	$3s3p^3(^2P^o)^3P^o3d$	$3s3p^3(^2P^o)^1P^o3d$	$3s3p^3(^2D^o)^3D^o3d$	$3s3p^3(^2D^o)^1D^o3d$	$3s^23p^2(^3P)4p$
	0.079 78	−0.110 10	−0.048 89	−0.012 84	−0.040 44
	$3s^23p^2(^1D)4f$	$3p^3(^2P^o)3d^2(^1S)$	$3p^3(^4S^o)3d^2(^1D)$	$3p^3(^2P^o)3d^2(^3P)$	$3p^3(^2D^o)3d^2(^1D)$
	−0.041 45	−0.031 04	−0.017 84	−0.019 54	0.008 64
	$3p^3(^2D^o)3d^2(^3P)$	$3s^23p^2(^1S)4p$	$3s3p^3(^2P^o)^1P^o4s$		
	−0.010 10	−0.007 15	0.008 88		

gular momentum of the continuum electron are included giving good convergence in energy range considered in the present work. The collisional description of the initial $S(^3P^e)$ bound state in the present R-matrix calculation gave the ionization energy of 0.747 06 Ry which is in good agreement with the observed value of 0.761 45 Ry of Kaufman.[7] The difference between the experimental and theoretical energy splittings will produce the shift in the position of resonances. The ionization thresholds have been adjusted to their experimental values to enable direct comparison between theory and experiment. In order to obtain the initial- and final-state wave functions in the entire configuration space, the differential equations in the external region which are coupled by long-range dipole and higher-multipole potentials are solved. the solutions are matched at the boundary using the R matrix, then the electric-dipole matrix elements and photoionization cross sections are calculated.

IV. RESULTS AND DISCUSSION

A. Partial and total cross sections

The total photoionization cross section is obtained by adding the partial contributions of $^3S^o$, $^3P^o$, and $^3D^o$ final states allowed by dipole selection rules. However, the $^3P^o$ final state will not contribute below the $^2D^o$ ionization threshold as it does not couple to the $^4S^o$ ground state of S^+. The length and velocity forms of the total cross sections are shown in Fig. 1 over the energy region between the first two ionization thresholds. The velocity form of the cross section lies below the length form, and they normally differ by about 15%. For the sake of clarity only the length form is shown at higher photon energies where the structure becomes narrow and complicated. The measured absolute values of Tondello[1] and Joshi *et al.*[4] are also shown. Joshi *et al.*[4] extended and improved the measurement of Tondello.[1] They obtained the relative photoionization cross section of atomic sulfur in the 1200–840-Å range using the flash-pyrolsis method. They

TABLE III. The calculated and experimental energies of the states of S^+ relative to the ground state.

State	Energy (a.u.) Experiment	Present work
$3s^23p^3\,^4S^o$	0.0	0.0
$3s^23p^3\,^2D^o$	0.06776	0.07630
$3s^23p^3\,^2P^o$	0.11189	0.12635

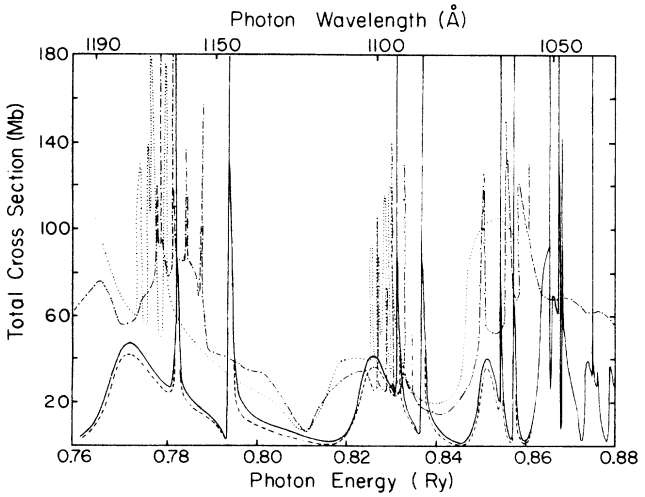

FIG. 1. The total cross section for photoionization of $S(^3P^e)$ ground state between the $^4S^o$ and $^2D^o$ thresholds. Solid curve, present length cross section; dashed curve, present velocity cross section; dotted curve, measured values of Tondello (Ref. 1); dashed-dotted curve, measured values of Joshi *et al.* (Ref. 4).

renormalized their cross section using absolute scale devised by Tondello. They have estimated an uncertainty of up to 30% in their values. The measured cross section of Tondello is not available from 1090 Å to the threshold. The present results remain lower than the measured over the entire energy range. The present results show some significant differences compared to the measured values. In particular, the average magnitude of the calculated cross sections differ significantly and the positions of the lower resonances are displaced as compared to the measurements. We have neglected the spin-orbit interaction in the present work. The inclusion of spin-orbit interaction will split the ground $3s^2 3p^4\,{}^3P^e$ state of sulfur to three ${}^3P^e_{0,1,2}$ levels and $3s^2 3p^3\,{}^4S^o$, ${}^2D^o$, and ${}^2P^o$ terms of S^+ will give rise to five ${}^4S^o_{3/2}$, ${}^2D^o_{3/2,5/2}$, and ${}^2P^o_{1/2,3/2}$ levels. The fine-structure effects give rise to additional Rydberg series of resonances starting from ${}^3P_2$ ground state and converging to the ionic state thresholds. Most of these series have been observed experimentally by Tondello,[1] Gibson *et al.*,[3] and Joshi *et al.*[4] In the most recent experiment, Joshi *et al.* have identified lines starting from ${}^3P_1$ and ${}^3P_0$ levels. The relativistic effects in the calculations can be included using relativistic R-matrix method.[20] However, these calculations do not seem to be feasible for sulfur as the correlation effects are very important and a large number of configurations need to be included in the expansion of the eigenstates. The relativistic effects are expected to be smaller than the correlation effects.

The photoionization spectrum is strongly perturbed by the autoionization structures. There are three Rydberg series of resonances converging to the ${}^2D^o$ threshold. The ${}^3S^o$ resonances are very narrow due to the weak coupling between the $3p^3({}^4S^o)\varepsilon s\,{}^3S^o$ continuum and the $3p^3({}^2D^o)nd\,{}^3S^o$ Rydberg states. There are two ${}^3D^o$ autoionizing Rydberg series occurring below ${}^2D^o$ threshold. One is narrow for a reason similar to that discussed above, while the other shows broad features due to the strong coupling between the $3p^3({}^4S^o)\varepsilon d\,{}^3D^o$ continuum and the $3p^3({}^2D^o)nd\,{}^3D^o$ Rydberg series. As pointed out by Gibson *et al.*,[3] the narrow features of the two resonance series occurring below the ${}^2D^o$ threshold can be explained on the basis of the fact that for the autoionization of these resonances the Rydberg orbital needs to change its angular momentum by two quanta which possibly slows down the autoionization process. The ${}^3P^e$-${}^3S^o$ and ${}^3P^e$-${}^3D^o$ partial photoionization cross sections in length form are shown in Figs. 2 and 3, respectively, in the photon energy range between the ${}^4S^0$ and ${}^2D^o$ thresholds. It is clear that the ${}^3P^e$-${}^3D^o$ partial cross section dominates in this energy region. In Figs. 1, 2, and 3 the peak cross sections for some members of the autoionized Rydberg series are truncated to 180 Mb. The ${}^3S^o$ partial cross section shows a simple structure superimposed on a weak background as compared to the ${}^3D^o$ partial cross section. Another prominent feature in the ${}^3D^o$ partial cross section is the strong perturbation of the $3p^3({}^2D^o)nd\,{}^3D^o$ Rydberg series by the presence of lower members of the $3p^3({}^2P^o)nd\,{}^3D^o$ autoionized Rydberg series converging to the ${}^2P^o$ ionization threshold which lies below the ${}^2D^o$ threshold.

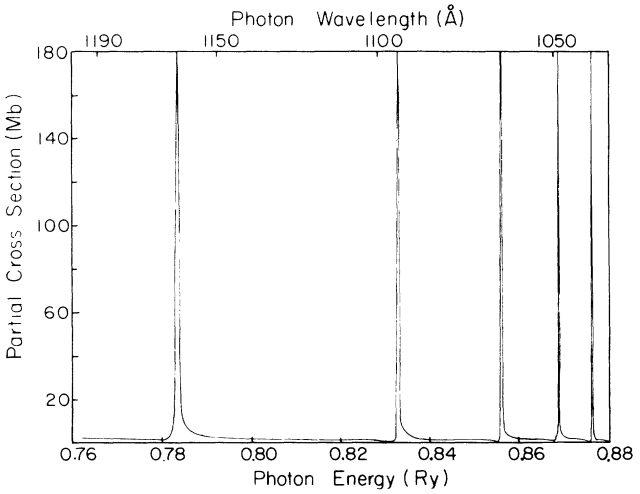

FIG. 2. The ${}^3S^o$ partial cross section in length form for the $S({}^3P^e)$ ground state between the ${}^4S^o$ and ${}^2D^o$ thresholds.

The length and velocity forms of the total photoionization cross section for photon energies from the ${}^2D^o$ threshold to 1.8 Ry is shown in Fig. 4. The experimental measurement of Tondello and Joshi *et al.* are also included. The cross section between the ${}^2D^o$ and ${}^2P^o$ thresholds contains three Rydberg series of resonances converging to the ${}^2P^o$ ionization threshold. Again the velocity form of the cross section lies below the length form and the measured values are higher than the present average theoretical results. However, the calculated peak values of the cross section are larger than the experiment. Above the ${}^2P^o$ ionization threshold, the cross section falls off rapidly with increase in photon energy. The length form of the ${}^3P^e$-${}^3P^o$ and ${}^3P^e$-${}^3D^o$ partial cross section are shown in Figs. 5 and 6, respectively. The ${}^3P^o$ partial cross section contains two $3p^3({}^2P^o)ns,md\,{}^3P^o$ Rydberg series of resonances while the ${}^3D^o$ partial cross section has $3p^3({}^2P^o)nd\,{}^3D^o$ resonances converging to the ${}^2P^o$ ion-

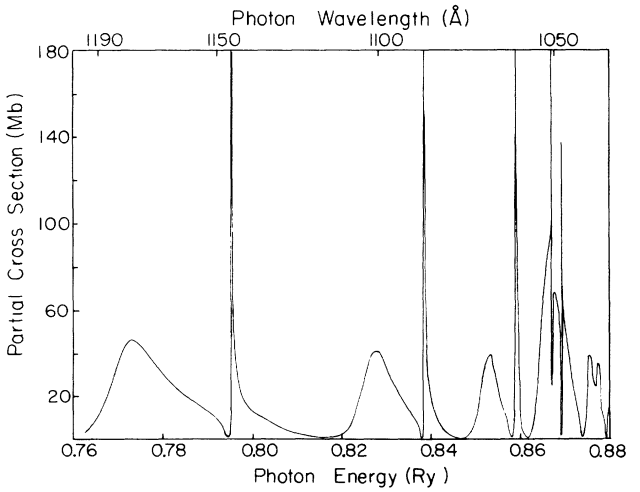

FIG. 3. The ${}^3D^o$ partial cross section in length form for the $S({}^3P^e)$ ground state between the ${}^4S^o$ and ${}^2D^o$ thresholds.

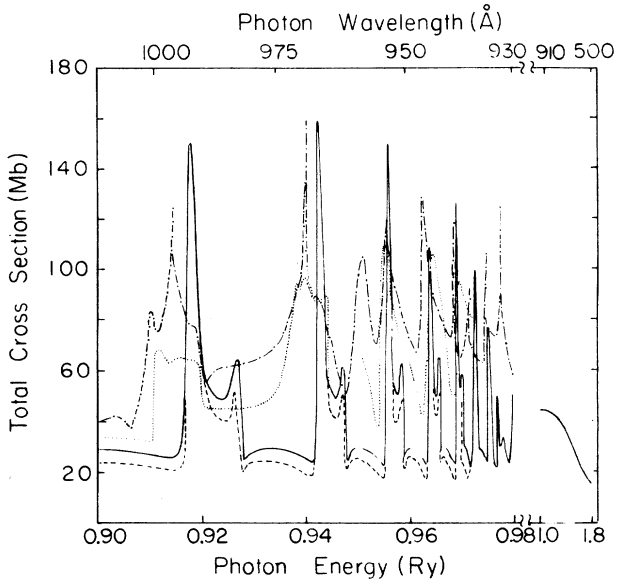

FIG. 4. The total cross sections for photoionization of the $S(^3P^e)$ ground state from the $^2D^o$ threshold to 1.8 Ry. Notations are as in Fig. 1.

ization threshold. The $3p^3(^2P^o)nd\ ^3D^o$ group of resonances are bigger and broader as compared to the $3p^3(^2P^o)nd\ ^3P^o$ resonances and the former almost lie over the latter. The background cross section for the $^3D^o$ partial wave are larger than for the $^3P^o$ partial wave. In Fig. 5 we have also shown the six-state close-coupling results of Mendoza (given in Berrington and Taylor[9]). We have calculated the partial photoionization cross sections leaving the ion in a particular state. We show the partial cross sections leaving the S^+ ion in the $^4S^o$ ground state and the first $^2D^o$ excited state in Fig. 7 in the energy range from the $^2D^o$ threshold to 1.8 Ry. The average magnitude of the $^2D^o$ partial cross section is approximately a factor of 2 larger than the $^4S^o$ partial cross section.

B. Autoionization levels

We have analyzed the lower members of the autoionized Rydberg series converging to the $^2D^o$ and $^2P^o$ states

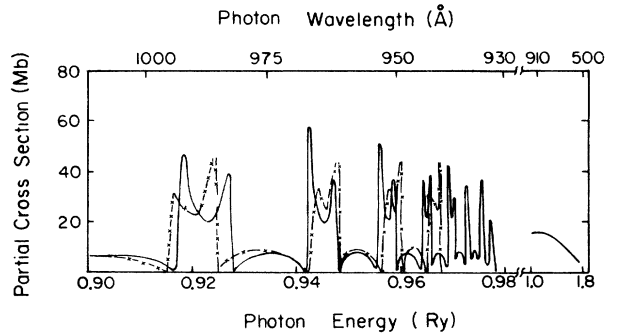

FIG. 5. The $^3P^o$ partial cross section in length form for the $S(^3P^e)$ ground state from the $^2D^o$ threshold to 1.8 Ry. Solid curve, present cross section; dashed-crossed curve, calculated values of Mendoza (Ref. 9).

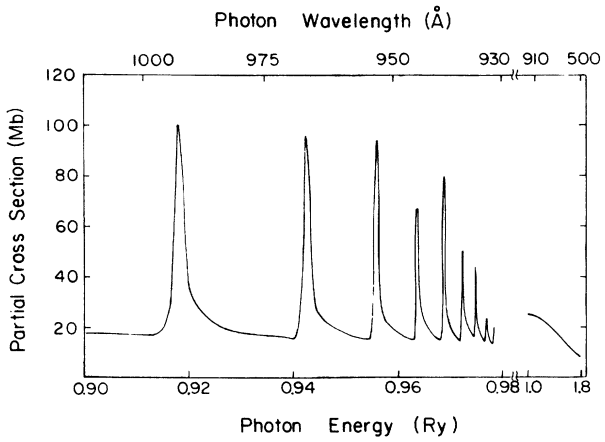

FIG. 6. The $^3D^o$ partial cross section in length form for the $S(^3P^e)$ ground state from the $^2D^o$ threshold to 1.8 Ry.

of the S^+ ion. The position and width of the resonances have been calculated using the resonance formula

$$\delta(E)=\delta_0+\tan^{-1}\left[\frac{\Gamma/2}{E-E_r}\right], \tag{5}$$

where δ_0 is the nonresonant background phase shift, Γ is the width, and E_r is the resonance position. In addition to position and width, each resonance is assigned an effective quantum number defined by

$$E_r(n)=-\frac{1}{n^{*2}} \tag{6}$$

The position, width, and effective quantum number of the resonances converging to the $^2D^o$ ionization threshold are presented in Table IV. The results of previous close-

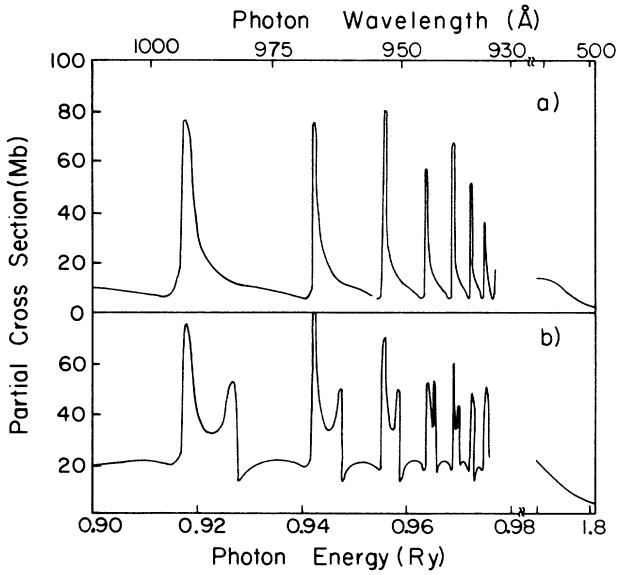

FIG. 7. The partial photoionization cross sections from the S ground state leaving the residual ions in the (a) $3s^23p^3\,^4S^o$ state and (b) $3s^23p^3\,^2D^o$ state as a function of photon energy from the $^2D^o$ threshold to 1.8 Ry.

TABLE IV. Parameters for the autoionizing series converging on $S^+(^2D^o)$ threshold in the photoionization of $S(^3P^e)$ ground state. The effective quantum number, n^*, is relative to the $^2D^o$ threshold. Numbers in square brackets denote powers of ten.

	Width (Ry)		Position (Ry)						Effective quantum number				
Designation	Present work	Conneely *et al.*[a]	Present work	Mendoza and Zeippen[b]	Conneely *et al.*[a]	Gibson *et al.*[c]	Joshi *et al.*[d]	Tondello[c]	Present work	Mendoza and Zeippen[b]	Conneely *et al.*[a]	Gibson *et al.*[c]	Joshi *et al.*[d]
$3p^3(^2D^o)3d\ ^3D^o$	1.39 [−2]	6.60 [−3]	0.771 04	0.769 21	0.775 28	0.763 15			2.818	2.798	2.865	2.730	
$3p^3(^2D^o)3d\ ^3S^o$	2.44 [−4]	5.39 [−4]	0.783 53	0.781 05	0.784 58	0.780 67	0.780 66	0.778 52	2.969	2.937	2.981	2.933	2.932
$3p^3(^2D^o)5s\ ^3D^o$	1.98 [−4]	9.33 [−4]	0.795 49	0.781 34	0.786 68	0.778 47	0.777 19	0.780 79	3.139	2.941	3.009	2.906	2.890
$3p^3(^2D^o)4d\ ^3D^o$	8.33 [−3]	5.31 [−3]	0.826 71	0.822 82	0.827 48	0.822 76			3.772	3.673	3.790	3.672	
$3p^3(^2D^o)4d\ ^3S^o$	1.31 [−4]	1.46 [−4]	0.833 06	0.831 79	0.834 18	0.832 68	0.832 72	0.830 98	3.956	3.917	3.986	3.946	3.946
$3p^3(^2D^o)6s\ ^3D^o$	3.20 [−5]	1.75 [−4]	0.838 52	0.833 22	0.836 08	0.830 94	0.831 08	0.832 74	4.137	3.961	4.048	3.893	3.897
$3p^3(^2D^o)5d\ ^3D^o$	4.60 [−3]	1.12 [−3]	0.852 83	0.850 30	0.851 15	0.851 19			4.760	4.629	4.666	4.677	
$3p^3(^2D^o)5d\ ^3S^o$	7.20 [−5]	1.19 [−4]	0.856 14	0.855 57	0.857 05	0.856 39	0.856 45		4.950	4.915	4.983	4.969	4.970
$3p^3(^2D^o)7s\ ^3D^o$	1.85 [−4]	3.01 [−4]	0.859 00	0.856 42	0.857 25	0.854 95	0.854 99		5.131	4.966	5.011	4.882	4.883
$3p^3(^2D^o)6d\ ^3D^o$	1.10 [−5]		0.866 93			0.866 68			5.770			5.742	
$3p^3(^2D^o)6d\ ^3S^o$	4.30 [−5]		0.868 68	0.868 35		0.868 89	0.868 82		5.946	5.916		5.993	5.964
$3p^3(^2D^o)8s\ ^3D^o$	2.50 [−5]		0.869 22			0.868 06	0.867 96		6.004			5.889	5.870
$3p^3(^2D^o)7d\ ^3D^o$	1.15 [−3]		0.874 55			0.875 32			6.680			6.728	
$3p^3(^2D^o)7d\ ^3S^o$	2.70 [−5]		0.876 23			0.876 66	0.876 67		6.944			7.030	7.026
$3p^3(^2D^o)8d\ ^3S^o$	8.69 [−4]		0.879 98			0.880 39			7.673			7.783	

[a]Reference 7.
[b]Reference 10.
[c]Reference 3.
[d]Reference 4.
[e]Reference 1.

TABLE V. Parameters for the autoionizing series converging on $S^+(^2P^o)$ threshold in the photoionization of $S(^3P^e)$ ground state. The effective quantum number, n^*, is relative to the $^2P^o$ threshold. Numbers in square brackets denote powers of ten.

	Width (Ry)		Position (Ry)						Effective quantum number				
Designation	Present work	Conneely *et al.*[a]	Present work	Mendoza and Zeippen[b]	Conneely *et al.*[a]	Gibson *et al.*[c]	Joshi *et al.*[d]	Tondello[e]	Present work	Mendoza and Zeippen[b]	Conneely *et al.*[a]	Gibson *et al.*[c]	Joshi *et al.*[d]
$3p^3(^2P^o)4d\ ^3P^o$	1.19 [−3]		0.918 13	0.913 95		0.914 40	0.914 03		3.861	3.746		3.759	3.750
$3p^3(^2P^o)4d\ ^3D^o$	1.74 [−3]		0.918 19	0.917 75		0.916 15			3.862	3.851		3.807	
$3p^3(^2P^o)6s\ ^3P^o$	1.01 [−3]	7.29 [−3]	0.927 02	0.921 45	0.923 25	0.920 41	0.920 43		4.145	3.961	4.013	3.930	3.931
$3p^3(^2P^o)5d\ ^3P^o$	6.96 [−4]	4.99 [−4]	0.942 49	0.940 55	0.941 75	0.940 74	0.940 29		4.837	4.730	4.789	4.745	4.722
$3p^3(^2P^o)5d\ ^3D^o$	1.01 [−3]	5.26 [−4]	0.942 63	0.942 55	0.943 35	0.941 91			4.845	4.840	4.878	4.809	
$3p^3(^2P^o)7s\ ^3P^o$	4.68 [−4]	4.31 [−4]	0.947 46	0.944 65	0.945 65	0.944 25	0.944 01		5.146	4.965	5.018	4.944	4.930
$3p^3(^2P^o)6d\ ^3P^o$	3.91 [−4]	4.05 [−4]	0.955 74	0.954 75	0.955 55	0.954 84	0.954 47		5.824	5.724	5.796	5.743	5.711
$3p^3(^2P^o)6d\ ^3D^o$	5.70 [−4]	4.62 [−4]	0.955 84	0.955 85	0.956 35	0.955 54		0.955 21	5.834	5.838	5.870	5.811	
$3p^3(^2P^o)8s\ ^3P^o$	2.89 [−4]	1.54 [−4]	0.958 73	0.957 15	0.957 75	0.956 25	0.956 73		6.144	5.968	6.008	5.944	5.932
$3p^3(^2P^o)7d\ ^3P^o$	2.66 [−3]		0.963 68			0.962 91	0.962 83		6.813			6.705	6.640
$3p^3(^2P^o)7d\ ^3D^o$	3.72 [−4]		0.963 77	0.963 85		0.963 52		0.963 28	6.827	6.839		6.799	
$3p^3(^2P^o)9s\ ^3P^o$	1.58 [−3]		0.965 61			0.964 34	0.964 20		7.141			6.930	6.909
$3p^3(^2P^o)8d\ ^3P^o$	1.79 [−4]		0.968 83			0.968 34	0.968 19	0.968 40	7.810			7.710	7.677
$3p^3(^2P^o)8d\ ^3D^o$	2.33 [−4]		0.968 90			0.986 75			7.826				7.806
$3p^3(^2P^o)10s\ ^3P^o$	7.40 [−5]		0.970 08			0.969 26			8.126			7.932	

[a]Reference 7.
[b]Reference 10.
[c]Reference 3.
[d]Reference 4.
[e]Reference 1.

coupling calculations of Conneely *et al.*[8] and Mendoza and Zeippen[10] and the experimental measurements of Tondello,[1] Gibson *et al.*,[3] and Joshi *et al.*[4] are included. As discussed in the introduction of the paper, Gibson *et al.* reversed the designation given by Tondello to the $3p^3(^2D^o)nd\ ^3S^o$ and $3p^3(^2D^o)ns\ ^3D^o$ levels. The present calculation agrees with the assignment of Tondello for these levels. There are two $^3D^o$ Rydberg series converging to the $^2D^o$ ionization threshold. The *s* member lies higher as a narrow companion to the broad *d* member. The effective quantum numbers of the lower members of all the three Rydberg series are larger than the experimental values, indicating a shift in the position of the autoionizing levels. The present results are in reasonable agreement with the previous calculations of Conneely *et al.*[8] and Mendoza and Zeippen.[10] Mendoza and Zeippen used a six-state ($3s^23p^3\ ^4S^o$, $^2D^o$, $^2P^o$, $3s3p^4\ ^4P$, ^2D, and $3s^23p^23d\ ^2P$) representation of the S^+ ion in their close-coupling calculations. The differences between the present results and the calculations of Mendoza and Zeippen may be due to the coupling effects to the excited channels and the difference in the basis functions used in the two calculations. The larger effective quantum number obtained in the present work for $3p^3(^2D^o)ns\ ^3D^o$ resonances as compared to the simple three-state close-coupling results of Conneely *et al.* is perhaps due to the adjustment of the calculated thresholds to the experimental values. The presence of the $3p^3(^2P^o)3d\ ^3D^o$ resonance below the $^2D^o$ threshold strongly perturbs the $3p^3(^2D^o)nd\ ^3D^o$ Rydberg series. It is the presence of this resonance which makes the width of the nearby $3p^3(^2D^o)6d\ ^3D^o$ resonance very narrow. In Table V, the resonance parameters of the three series of resonances converging to the $^2P^o$ threshold are compared with the experimental results of Joshi *et al.*,[4] Gibson *et al.*,[3] and Tondello[1] and the calculations of Conneely *et al.*[8] and Mendoza and Zeippen.[10] The width of the $3p^3(^2D^o)nd\ ^3D^o$ resonances converging to the $^2D^o$ are bigger than the $3p^3(^2P^o)nd\ ^3D^o$ resonances converging to the $^2P^o$ threshold.

To summarize, in the present work the initial state $S(^3P^e)$ and the final continuum states $S^+ + e^-(^3S^o, ^3P^o, ^3D^o)$ are described consistently by the *R*-matrix expansions over the three ionic states $S^+(3s^23p^3\ ^4S^o, ^2D^o, ^2P^o)$. The present results are compared with the measurements of Tondello, Gibson *et al.*, and Joshi *et al.* and the previous close-coupling calculations of Conneely *et al.*, and Mendoza and Zeippen. The present results show some significant departures from the measurements. The discrepancy between the present results and the measurements can mainly be attributed to the description of the S^+ ionic states and omission of spin-orbit interaction. In addition, we have restricted the collisional expansions to the $3p$ ejection channels. The accuracy of the calculation can perhaps be improved by choosing more flexible bound orbitals and large number of configurations to represent the S^+ states. Furthermore, in order to take a proper account of channel mixing the $3s$ ejection channels should be included in the collisional expansions. Finally, the relativistic terms should be included in the Hamiltonian for a more meaningful comparison with the recent accurate experiments.

ACKNOWLEDGMENTS

It is a pleasure to thank Dr. Ronald J. W. Henry for his help and encouragement and Dr. A. R. P. Rau for his helpful comments. This work is supported by the National Aeronautics and Space Administration Grant No. NAGW-48.

[1]G. Tondello, Astrophys. J. **172**, 771 (1972).
[2]V. N. Sarma and Y. N. Joshi, Physica **123C**, 349 (1984).
[3]S. T. Gibson, J. P. Greene, B. Rusek, and J. Berkowitz, J. Phys. B **19**, 2825 (1986).
[4]Y. N. Joshi, M. Mazzoni, A. Nencioni, W. H. Parkinson, and A. Cantu, J. Phys. B **20**, 1203 (1987).
[5]Y. G. Toresson, Ark. Fys. **18**, 417 (1960).
[6]J. F. Alder, R. M. Bombelka, and G. F. Kirkbright, J. Phys. B **11**, 235 (1978).
[7]V. Kaufman, Phys. Scr. **26**, 439 (1979).
[8]M. J. Conneely, K. Smith, and L. Lipsky, J. Phys. B **3**, 493 (1970).
[9]K. A. Berrington and K. T. Taylor, Comput. Phys. Commun. **26**, 397 (1982).
[10]C. Mendoza and C. J. Zeippen, J. Phys. B **21**, 259 (1988).
[11]A. L. Broadfoot, B. R. Sandel, D. E. Shamansky, J. C. McConnell, G. R. Smith, J. B. Holberg, S. K. Atreya, T. M. Donahue, D. F. Strobel, and J. L. Bertaux, Geophys. Res. **86**, 8259 (1981).
[12]D. E. Shemansky and G. R. Smith, Geophys. Res. **86**, 9179 (1981).
[13]S. S. Tayal, Ronald J. W. Henry, and S. Nakazaki, Astrophys. J. **313**, 487 (1987).
[14]P. G. Burke and W. D. Robb, Adv. At. Mol. Phys. **11**, 143 (1975).
[15]P. G. Burke and K. T. Taylor, J. Phys. B **8**, 2620 (1975).
[16]E. Clementi and C. Roetti, At. Data Nucl. Data Tables **14**, 177 (1974).
[17]A. Hibbert, Comput. Phys. Commun. **9**, 141 (1975).
[18]J. E. Petterson, Phys. Scr. **28**, 421 (1983).
[19]K. A. Berrington, P. G. Burke, M. Le Dourneuf, W. D. Robb, K. T. Taylor, and Vokylan, Comput. Phys. Commun. **14**, 367 (1978).
[20]N. S. Scott and K. T. Taylor, Comput. Phys. Commun. **25**, 347 (1982).